

# Diameter-dependent annealing kinetics of X-ray-induced defects in single-walled carbon nanotubes

T Murakami<sup>1</sup>, M Matsuda<sup>1</sup>, S Isozaki<sup>1</sup>, K Kisoda<sup>2</sup> and C Itoh<sup>1</sup>

<sup>1</sup>Department of Materials Science and Chemistry, Wakayama University, Wakayama 640-8510, Japan

<sup>2</sup>Department of Physics, Wakayama University, Wakayama 640-8510, Japan

E-mail: murakami@sys.wakayama-u.ac.jp

**Abstract.** Diameter-dependent annealing effects of X-ray-induced defects in single-walled carbon nanotubes (SWNTs) were studied by Raman scattering spectroscopy. We found that X-ray-induced defects were formed in thin SWNTs at higher density than that in thick SWNTs. The X-ray-induced defects, distant pairs of interstitials and vacancies (I-V), were eliminated by thermal annealing. The recovery temperature of the X-ray-induced defects in the thin SWNTs were higher than that of the thick ones, indicating the thermal stability of the defects in thinner SWNTs are higher. In order to simulate the annealing behaviours of the X-ray-induced defects in SWNTs with diameters of  $\sim 0.9$  and  $\sim 1.4$  nm, we suggested the competitive reactions of diffusion of interstitials, formation of close I-V pairs and their recombination. The simulated results showed that the reaction-rate constant of elimination of close I-V pairs is dependent on tube diameter, which is presumably derived from nano-structure effects of SWNTs.

## 1. Introduction

Single-walled carbon nanotubes (SWNTs) have characteristic electric properties originated from quasi-one-dimensional structure.[1] Their electronic property strongly depends on chirality, which describes “how to roll up” the 2D graphite sheet to make the SWNT. Because of this strong correlation between the electronic structure and the geometric structure, structural modification is one of the most feasible methods for controlling their electronic properties. However their chemical stability and mechanical toughness impede their structural modification. One of the feasible methods for modifying SWNT’s structure is to utilize the defect formation induced by ionizing radiation.[2-4] Hirahara *et al* showed that the defect migration changed the chirality of a tube under the simultaneous application of tensile stress and heat by transmission electron microscope.[5] We also reported that X-ray irradiation formed distant interstitial-vacancy pairs in SWNTs, and the accumulation of the defects eventually resulted in modification of their structure.[6,7] This phenomenon is potentially available to control the SWNT’s structure. In order to develop the structural modification method based on the irradiation effect, we should elucidate characteristics of the irradiation-induced defect in SWNTs. Since the SWNT samples used in our previous study [6] had wide diameter distribution, the observed results were the ensemble average over different tubes. The wide diameter distribution may veil the dependence of the defect process on the tube diameter.

In the present report, we show the results of the study on thermal annealing kinetics of the X-ray-induced defects in SWNTs with narrow diameter distributions, and discussed their thermal stability in terms of the tube diameter. We found that the X-ray irradiation induced defects at higher density in



thinner tube and complete recovery of the X-ray-induced defect required higher sample temperature in thinner tube. The recovery process of the defects was hardly explained by a simple diffusion-limited recombination, and thus we made a simulation with considering competitive-recovery reactions composed of diffusion-limited recombination and the reaction involving formation of intermediate state, like close I-V pair. The results showed that the reaction-rate constant of elimination of close I-V pairs was dependent on tube diameter. The diameter dependence of the annealing effect is presumably derived from nano-structure effects of SWNTs.

## 2. Experimental procedure

SWNT samples synthesized by arc-discharge technique and CoMoCAT CVD method were purchased from Aldrich Co., Ltd. Their mean diameters were  $\sim 1.4$  and  $0.9$  nm, evaluated by Raman measurements. The purchased SWNTs were dispersed in aqueous solutions of 1-wt% sodium dodecyl sulfate using a tip-type sonicator. The dispersed solutions were centrifuged, and then the supernatant filtered using a mixed cellulose ester membrane. After the membrane was removed by acetone, the SWNT films were transferred on silicon substrates. The SWNT films were irradiated with X-ray (1.24 keV) in vacuum. The irradiated samples were taken in the air and subsequently annealed at the given temperatures for 30 min. The annealing temperature was raised sequentially in each annealing from 100 to 700 °C by the step of 50-100 °C. The irradiated and annealed SWNT samples were characterized by Raman scattering spectroscopy at room temperature using a probe laser of 532 nm.

## 3. Results and Discussion

Figure 1 shows the Raman spectra of the pristine, irradiated, and annealed (600 °C) SWNTs synthesized by (a) arc-discharge technique and (b) CoMoCAT CVD method. Tangential vibration modes of  $\sim 1600$   $\text{cm}^{-1}$  (G band) and defect-induced mode of  $\sim 1350$   $\text{cm}^{-1}$  (D band) are clearly observed for both samples. The Raman intensities were normalized with respect to the G band. Insets in Fig. 1(a) and (b) show radial breathing modes (RBMs) of pristine samples. The diameter of SWNT ( $d$ ) can be estimated from RBM frequency ( $\omega_{\text{RBM}}$ ). [8] We evaluated  $d \sim 1.4$  and  $\sim 0.9$  nm from the observed peaks of  $\omega_{\text{RBM}} \sim 170$  and  $\sim 270$   $\text{cm}^{-1}$ , respectively. Hereafter, we describe the SWNT of  $d \sim 1.4$  nm as the thick tube and describe the SWNT of  $d \sim 0.9$  nm as the thin tube.

X-ray irradiation enhanced the intensity of the D band, indicating that the irradiation induced defects in SWNTs. We found that the D band enhancement of the thin tube was much larger than that of the thick tube. This result shows the thicker tube is more tolerant to the radiation. The increases in the D band intensity of both irradiated samples were reduced by annealing at 600 °C. This recovery was ascribed to the recombination of vacancy and interstitial pair. While the net increase of the D band in thick tube recovered by the annealing, that of the thin tube did not fully recover even at the maximum annealing temperature in the present study. The slight changes of the Raman spectra are possibly related to the modification of tube structure by the X-ray irradiation and subsequent annealing.

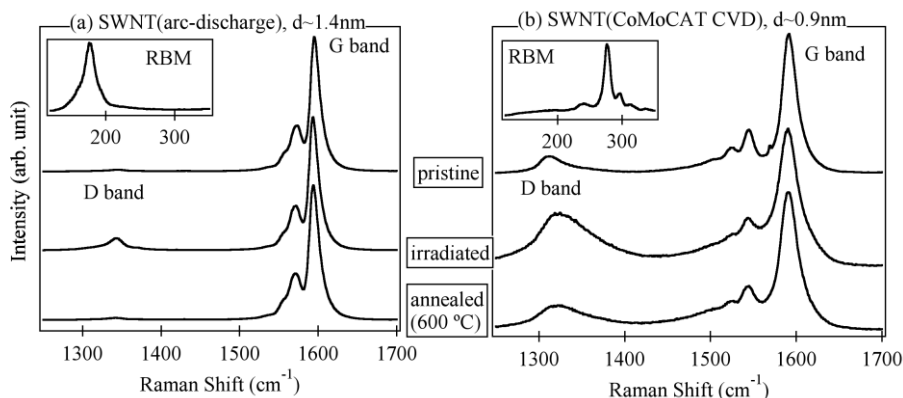


**Figure 1.** Raman spectra of pristine, irradiated, and annealed SWNTs of (a)  $d \sim 1.4$  nm and (b)  $d \sim 0.9$  nm. Insets show RBMs of pristine samples.

In Fig. 2, we plotted the ratio of the changes in the net increase of D band by the X-ray irradiation to G band ( $\Delta D/G$ ) as a function of the annealing temperature. The annealing behaviors of each tube are remarkably different in two aspects: the completing temperature of the annealing and the magnitude of a hump in the annealing profile around 300 °C. While  $\Delta D/G$  of thick tube almost faded out near 400 °C, that of thin tube showed decrease up to 600 °C. This results shows that the defects formed in the thin tube are more stable than those in the thick tube. The annealing profiles of each tube showed a broad hump ranging from 200 °C to 400 °C. The magnitude of the hump is larger in the thin tube than the thick tube. The results suggest that the defect recovery process is not simple and depends on the tube diameter.

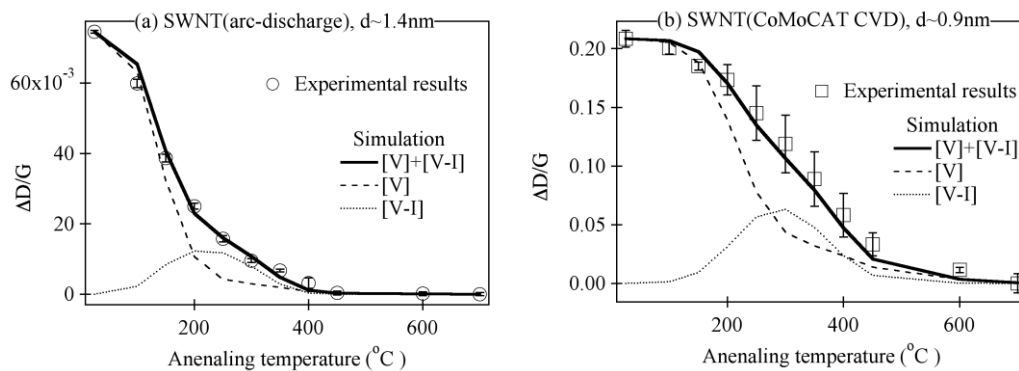
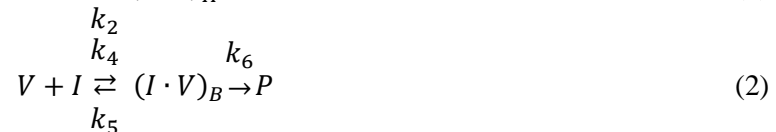


**Figure 2.**  $\Delta D/G$  of SWNTs with diameter of (a)  $\sim 1.4$  nm and  $\sim 0.9$  nm, depending on annealing temperature. Solid, dashed, and dotted lines show the simulated results.

The X-ray-induced defect in SWNT has a form of distant vacancy-interstitial pair.[6] Hence, the recombination of the defect is controlled by diffusion process. Our previous study using SWNT samples with wide diameter distribution showed the defect-recovery process was successfully simulated by a 2nd-order reaction model.[6] The simple simulation used in our previous study hardly explains the hump found in the present study. Since the samples used in our previous study were mixture of SWNTs with various diameters, the observed signals were ensemble average of the signals of each SWNT. Hence, the detail annealing features depending on the tube diameter were probably averaged out.

In order to explain the annealing profiles obtained in the present study, we presume that intermediate states are formed prior to the interstitial-vacancy (I-V) recombination. One of the most probable candidates for the intermediate state is close I-V pair. When the close I-V pair instantaneously recombines after the formation, the pair formation process dominates the recombination reaction. However, the recombination rate is much slower than the pair formation rate, the recombination of the close pair is the rate-determining process. In SWNT, it is possible that the recombination rate of the close pair depends on the configuration of the pair. Thus, we presume that two types of close I-V pairs are formed as the intermediate states: one has a recombination rate much larger than the formation rate and the other has a recombination rate smaller than the formation rate. The reaction schemes are described below:



Here, V, I, and P denote a vacancy, an interstitial, and a perfect lattice in an SWNT, respectively. Two close I-V pairs are designated as  $(I \cdot V)_A$  and  $(I \cdot V)_B$ .  $k_i$  ( $i=1,2,3,4,5,6$ ) are the reaction rate constants. Thermal activation type temperature dependence of the reaction rate constants,  $k_i = k_{0i} \exp(-E_{ai}/k_B T)$ , is considered.  $k_{0i}$ ,  $E_{ai}$ , and  $k_B$  are pre-exponential factors, activation energies, and Boltzmann constant,

respectively. Based on our presumption, we set the conditions  $k_1 \ll k_3$  and  $k_6 \ll k_4$ . The former condition provides that the formation of (I-V)<sub>A</sub> is the rate-determining process of the reaction scheme (1), and the later provides that the recombination of (I-V)<sub>B</sub> is the rate-determining process of the scheme (2). Consequently, the reaction velocities are described as bellow differential equations.

$$\frac{d[V]}{dt} = -(k_1 + k_4)[V][I] + k_5[I \cdot V] = -(k_1 + k_4)[V]^2 + k_5[I \cdot V] \quad (3)$$

$$\frac{d[I \cdot V]}{dt} = k_4[V][I] - (k_5 + k_6)[I \cdot V] = k_4[V]^2 - (k_5 + k_6)[I \cdot V] \quad (4)$$

[V], [I], and [I-V] are the densities of the vacancy, the interstitial, and the close I-V pair in SWNTs, respectively. Because the X-ray-induced defects composed of vacancy and interstitial, [V] is equal to [I].  $\Delta D/G$  are generally proportional to the defect density.[9] In the present simulation, we suppose that all of the vacancies contributes  $\Delta D/G$  equally. Hence,  $\Delta D/G$  is proportional to the sum of [V] and [I-V]. We optimized parameters of  $k_1$ ,  $k_4$ ,  $k_5$ ,  $k_6$  and simulated using numerical analytical approach. The simulated results are shown as the solid curves in Fig. 2. The result shown in the figure is one of the results successfully reproducing the experimental points. The dashed and dotted curves show the contributions of [V] and [I-V], respectively. While [V] is dominated by the interstitial diffusion, [V-I] is governed by the recombination of close I-V pair. In order to simulate the annealing profile of the thin tube, we suppose the larger contribution of close I-V pair in the thin tube than that in the thick tube. Presumably,  $k_6$  depends on the tube diameter and the dependence is derived from nano-structure effects of SWNTs. The local configuration of I-V pair would be affected by curvature of the wall. This curvature effect is stronger in the thin tube than thick tube.

On the basis of these results, we suggest that the recombination of distant I-V pair involves formation of intermediate state, like close I-V pair. In the present study, we cannot determine the best parameters of  $k_{oi}$  and  $E_{ai}$ , because many parameters were used in our simulation. In order to reveal the tube-diameter dependence of these parameters, further approaches are required such as an isothermal annealing experiment, direct observation of the defects using TEM or atomic force microscope, and theoretical calculations.

#### 4. Conclusion

Diameter-dependent annealing kinetics of the X-ray-induced defects in SWNTs was studied by Raman scattering spectroscopy. The thermal stability of the X-ray-induced defects in thin SWNTs ( $d \sim 0.9$  nm) were higher than those of thick SWNTs ( $d \sim 1.4$  nm). The annealing profiles of these tubes were explained by concerning the formation of intermediate states, like close I-V pairs. The yield of the intermediate state depends on tube diameter; the I-V pairs' elimination in thick SWNTs has the higher reaction-rate constant than that in thin SWNTs. In order to clarify the recovery reaction of the X-ray-induced defects in detail, further experimental and theoretical studies are required.

#### References

- [1] Rotkin S V and Sunramoney S 2005 *Applied Physics of Carbon Nanotubes: Fundamentals of Theory, Optics and Transport Devices* (Springer: Berlin) p 227
- [2] Pomoell J A V, Krashennnikov A V, Nordlund K and Keinonen J 2004 *J. Appl. Phys.* **96** 2864
- [3] Suzuki S and Kobayashi Y 2007 *J. Phys. Chem. C* **111** 4524
- [4] Itoh C, Uotome K, Kisoda K, Murakami T and Harima H 2008 *Nucl. Instrum. Methods Phys. Res., Sect. B* **266** 2772
- [5] Hirahara K, Inose K and Nakayama Y 2010 *Appl. Phys. Lett.* **97** 051905
- [6] Murakami T, Yamamoto Y, Kisoda K and Itoh C 2013 *J. Appl. Phys.* **114** 114311
- [7] Murakami T, Yamamoto Y, Matsuda M, Kisoda K and Itoh C 2014 *Jpn. J. Appl. Phys.* **53** 02BD11
- [8] Jorio A, Saito R, Hafner J H, Lieber C M, Hunter M, McClure T, Dresselhaus G and Dresselhaus M S 2001 *Phys. Rev. Lett.* **86** 1118
- [9] Cançado L G, Jorio A, Ferreira E H M, Stavale F, Achete C A, Capaz R B, Moutinho M V O, Lombardo A, Kulmala T S and Ferrari A C 2011 *Nano Lett.* **11** 3190